Size-Dependent Carbon Monoxide Adsorption on Neutral Gold Clusters

N. Veldeman,[†,‡] P. Lievens,[†] and M. Andersson*[,‡]

Laboratorium voor Vaste-Stoffysica en Magnetisme, K.U.Leuven, Celestijnenlaan 200D, B-3001 Leuven, Belgium, and Department of Experimental Physics, Chalmers University of Technology and Göteborg University, SE-412 96 Göteborg, Sweden

Received: October 1, 2005

We report on experiments probing the reactivity of neutral Au_n clusters, $n = 9-68$, with carbon monoxide. The gold clusters are produced in a pulsed laser vaporization cluster source, operated at room temperature (RT) or at liquid-nitrogen temperature (LNT), pass through a low-pressure reaction cell containing CO gas, and are subsequently laser ionized. The reaction probabilities are determined by recording mass abundance spectra with time-of-flight mass spectrometry. The main observations are a strong temperature dependence and a remarkable size dependence. Upon cooling of the cluster source to LNT, the reactivity increases substantially. At LNT, the reaction probabilities for Au_n with the first CO molecule are about a factor 10 higher than at RT. Moreover, adsorption of two, three, and even four CO molecules is observed, in contrast to RT clusters which at most adsorb one CO molecule. This temperature dependence is related to the lifetime of the cluster-molecule complexes, being much longer for cold clusters. The observed striking size dependence is similar at both temperatures and is discussed in terms of the electronic structure effects.

Introduction

Gold nanoclusters recently have attracted a rapidly growing interest for a variety of reasons. First, gold as a coinage metal is interesting because of its specific electronic structure. It has the atomic configuration [Xe] $4f^{14}5d^{10}6s^1$ and therefore is classified as a transition metal. On the other hand, gold shows properties similar to alkali metals due to its single valence *s* electron. The delocalization of these valence electrons gives rise to a shell structure, resulting in the appearance of so-called magic numbers, corresponding to electronic shell closures.[1−3] For pure gold clusters, the shell closings occurring for clusters with 2, 8, 18, 20, 34, 58, etc. delocalized valence electrons are reflected in cluster properties such as stability, electron affinity, ionization potentials, and ionization efficiency.[4−9] Second, gold clusters have been found to adopt geometries different from clusters of most other metals. Two-dimensional structures have been observed or predicted as the most stable isomers for anionic and neutral gold clusters up to a size of around 13 atoms.[10−13] For Au_{20} there is experimental evidence for a tetragonal structure,[14] and a cage structure has been proposed for Au_{32}.[15] In the 20- to 60-atom size range also chiral and low-symmetry structures have been predicted,[16] and recent experimental results have also been interpreted in this direction.[17] Third, nanoscale gold particles are extremely interesting due to their potential use as nanocatalysts to many reactions. Although gold is almost chemically inert as bulk material, supported nanosize gold particles are found to show a remarkable catalytic activity for many reactions, such as CO combustion, propylene epoxidation, NO_x reduction, methanol synthesis, and water-gas shift.[18−22] Despite the importance of heterogeneous catalysis by nanoscale gold particles, the reasons for the enhancement of catalytic activity are not yet completely understood.

Several studies on the reactivity of gold clusters have been reported previously. The major part of the gold nanoparticles research is attributed to the investigation of the reactivity of deposited gold clusters. Several attempts have been made to clarify the catalytic behavior shown by small gold particles supported on metal oxides. In those investigations, attention is especially drawn to the size and support dependence, to the oxidation state of the active gold species, and to the possible mechanisms involved in the reactions.[23−32] Apart from experimental research, also theoretical work on supported gold nanoclusters has recently been done: calculations on structural, electronic, and impurity-doping effects were performed.[24,33−37]

As an understanding of the involved mechanisms remains a challenge, also the reactivity of gas-phase gold clusters toward reactants of interest needs to be investigated. Several coadsorption studies have been carried out,[38−42] and in some cases experimental evidence for catalytic formation of CO_2 was found.[39,40,43,44] However, most studies on the free clusters deal with the reactivity toward one specific molecule, and O_2 is probably the most extensively investigated. With the exception of Au_{10}^+, O_2 was found to only adsorb onto anionic Au_n with even *n*.[39,40,45−48] The higher reactivity of the odd-electron gold clusters can be explained by a more efficient charge transfer from the singly occupied orbital of the gold cluster into the singly occupied π^* orbitals of O_2. In addition, the charge transfer is expected to be facilitated by a lower electron affinity of the odd-electron clusters. This mechanism of oxygen bonding to gold clusters has also essentially been verified and further quantified in computational studies.[49−53] When an odd-electron species such as OH was preadsorbed onto the gold cluster anions, the odd−even pattern in *n* was reversed so that the Au_nOH^- with odd *n* and an odd number of electrons became the more reactive ones.[52] An odd−even variation was also found in the H_2S reactivity with Au_n^+ with odd-electron clusters being more reactive, in most cases to form Au_nS^+.[54] For methane and H_2 adsorption onto Au_n^+, there are significant size-to-size

* To whom correspondence should be addressed. E-mail: Mats.Andersson@fy.chalmers.se.
† K.U. Leuven.
‡ Chalmers University of Technology and Göteborg University.

10.1021/jp0556097 CCC: $30.25
Published on Web 11/22/2005

fluctuations and an overall trend of decreasing reactivity with increasing size up to $n = 15$.[45] Larger sizes appeared unreactive. In the same study H_2 was found to adsorb only onto two sizes $n = 3$ and 7 of neutral Au_n and to none of the anions. Computational studies also include investigations of the adsorption of molecular hydrogen,[55] atomic hydrogen,[56−58] or propene.[59] The focus of the studies of methanol and ethanol adsorbed onto gold clusters has been to characterize the bond character and the vibrational frequency of the adsorbed molecules.[60−63]

The experimental investigations of CO on gold clusters have so far been restricted to ionic species,[39,40,46,64−69] except for an investigation of the neutral dimer.[70] In contrast to the CO reactivity of most transition metal clusters,[71−78] which with only a few exceptions such as Al,[72,79] Co,[78] and Cu,[46,64,72,80,81] exhibit a relatively weak cluster size dependence above a threshold size, pronounced size-variations in the CO adsorption efficiency was detected for the gold cluster ions. In computational studies properties such as adsorption geometries, binding energies, and vibrational frequencies have been calculated for small gold clusters of different charge states.[42,58,69,82] By performing CO adsorption studies on neutral gold clusters in the gas phase, we aim at providing important information regarding the size, shape, and electronic structure dependence in order to extend the knowledge gained from the reactivity experiments on ionic clusters, to reveal further details of the reaction and bonding mechanisms.

In this paper we report on reactivity experiments on neutral Au_n clusters with CO. The reactivity is measured with the cluster source at room temperature (RT) and liquid-nitrogen temperature (LNT) and found to be considerably higher at the lower temperature. This temperature dependence is ascribed to the stabilization of the reaction products, this in turn related to comparison of binding energy and internal thermal energy of the cluster. Furthermore, the reactivity is found to exhibit similar size dependent behavior at both temperatures. The observed reaction probabilities point at electronic properties governing this effect: counting the number of delocalized electrons in reacted species reveals a correlation between reactivity and cluster electronic shell closings, and odd−even staggering in the reaction probabilities as a function of the number of atoms is observed.

Experimental Methods and Data Evaluation

A. Cluster Production and Mass Spectrometry. A detailed description of the employed setup and methods for evaluation of the reaction probability in cluster-reactivity experiments is given elsewhere.[83] Here only a brief overview will be given. The experimental setup is shown in Figure 1. It consists of two vacuum chambers, one for cluster production and the other one for the detection of the clusters.

The clusters are produced in a pulsed laser vaporization source. A high-energy laser pulse (third harmonic of a Nd:YAG laser, 355 nm) vaporizes the surface of a solid metal disk, which is continuously rotated and translated. Simultaneously, a high-pressure inert gas pulse is introduced into the source, inducing cooling of the hot metal vapor plume and initiating cluster aggregation. Subsequently, the mixture of atoms, clusters, and inert gas is expanded into vacuum and enters the second chamber through a 1 mm diameter skimmer, which skims off most of the helium and defines a narrow cluster beam.

In the second chamber, the cluster beam passes through the reaction cell, which contains the reactive gas at room temperature. The cell is cylindrical, 6 mm in diameter, and 50 mm long and has a 1 mm entrance and a 1.2 mm exit aperture. The small apertures ensure a high pressure ratio ($>10^3$) between the reaction cell and the surrounding chamber, preventing collisions with gas molecules outside the cell. In the experiment, CO gas was leaked into the reaction cell, maintaining a pressure in the cell in the range 1×10^{-2} to 1×10^{-1} Pa. The pressure was measured by a capacitance gauge on the gas inlet tube and corrected for the pressure drop between the measuring point and the reaction cell. At the applied pressures, the average number of collisions experienced by the clusters during their passage through the cell is less than five. The actual number of collisions for the individual clusters follows a Poisson distribution.

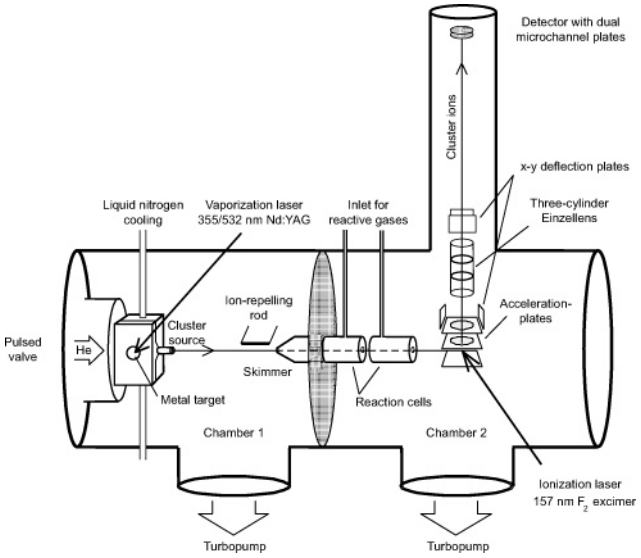

Figure 1. The cluster beam experimental setup.

After passing through the cell, the beam enters the ionization and detection region. To achieve efficient ionization of the gold clusters, 7.89 eV photons from a F_2 excimer laser were used, and a filter was introduced to block the red light in the ionizing photon beam. The intensity was kept low to minimize multiphoton absorption, and no evidence of CO desorption or fragmentation was observed at the used intensities, i.e., the ratio between pure and reacted clusters was independent of the laser light intensity and no odd−even variations in the total abundance were observed. The clusters were detected in a linear time-of-flight mass spectrometer with mass resolution, $M/\Delta M$, 300.

The laser vaporization source is operated at room temperature or at liquid-nitrogen temperature. The exact cluster temperature is not known, but is assumed to be approximately the temperature of the cluster source. Since temperature is an important factor in cluster reactivity experiments, cluster source parameters were carefully optimized for stable production and good thermalization. The temperature of the cluster source also affects the beam velocity, which is estimated to 1500 and 700 m/s for the source at RT and LNT, respectively. This corresponds to average center-of-mass impact energies of 0.25 and 0.07 eV for the collisions with CO molecules in the reaction cell.

For evaluation of the reaction probability, we recorded mass spectra at about 20 different pressures of CO gas in the reaction cell, for both source temperatures.

B. Models and Procedures for Data Evaluation. Initially there is one peak for each cluster size in the mass spectra, and when introducing the reactive gas in the reaction cell, additional peaks appear, as can be seen in Figure 2, showing mass spectra of Au_n clusters produced at LNT and reacted with CO molecules. $Au_n(CO)_m$ species are indicated as (n,m). Bare

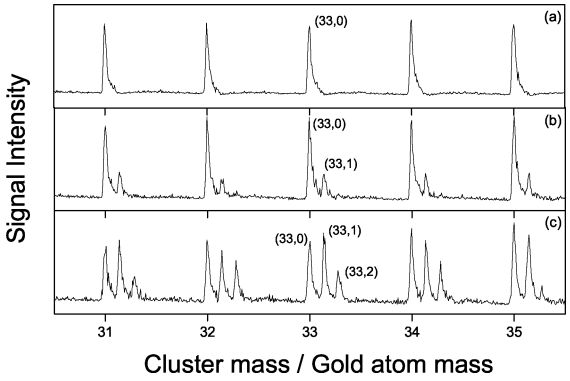

Figure 2. Mass spectra of Au_n clusters ($n = 31-35$) produced at LNT and reacted with CO. The $Au_n(CO)_m$ species are indicated as (n,m). (a) No CO in the reaction cell. Only pure Au_n clusters are observed. (b) 0.032 Pa CO in the reaction cell. The first ($m = 1$) reaction product with CO can be observed, shifted to the right of the bare cluster peak. (c) 0.098 Pa CO in the reaction cell. First ($m = 1$) and second ($m = 2$) reaction products can be observed.

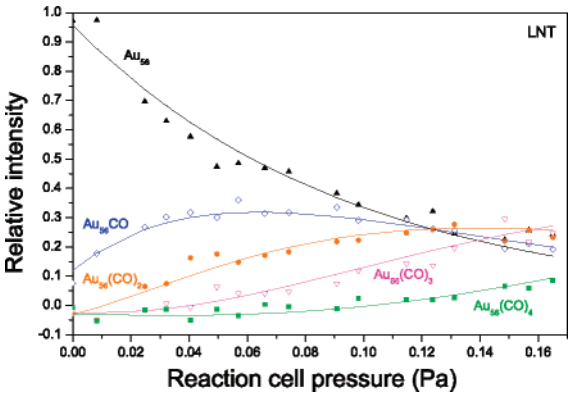

Figure 3. Relative abundance of Au_{56} (▲) and its reaction products $Au_{56}CO$ (◇), $Au_{56}(CO)_2$ (●), $Au_{56}(CO)_3$ (▽), and $Au_{56}CO_4$ (■) as a function of cell pressure, produced at LNT. The lines represent fits with a pseudo-first-order kinetic model.

clusters ($m = 0$) as well as clusters with CO molecules adsorbed ($m > 0$) can be observed. The relative abundance of pure and reacted clusters can, thus, be determined for each CO pressure in the reaction cell.

Under few-collision conditions, where each collision is regarded as an individual event, the successive addition of adsorbed molecules can be described with a statistical pseudo-first-order kinetic model.[83] To evaluate the reactivity, the relative abundance of clusters with 0, 1, 2, 3, or up to 4 adsorbed molecules is plotted vs cell pressure, or average number of collisions, and the kinetic expressions are fitted to the experimental data, as illustrated in Figure 3, showing the kinetic model fitting for Au_{56} produced at LNT. The fitting parameters are the individual reaction probabilities, S_1, S_2, S_3, and S_4 for the successive adsorption of the first, second, third, and fourth molecule.

The average number of collisions experienced by a cluster passing through the cell at a certain pressure is determined using the ideal gas law and assuming a hard-sphere model for the cross-section of the clusters and the CO molecules. The hard-sphere radius of the cluster, R_n, is calculated by assuming that the cluster has the same density as the bulk metal and by adding a constant value, d, to account for surface roughness and interaction outside the hard-core cross-section. The radius of a cluster consisting of n atoms is thus $R_n = n^{(1/3)}r_b + d$. Herein r_b is the radius of an atom with bulk metal density, 1.59 Å for gold. For the correction factor d, we used a typical value of 0.5

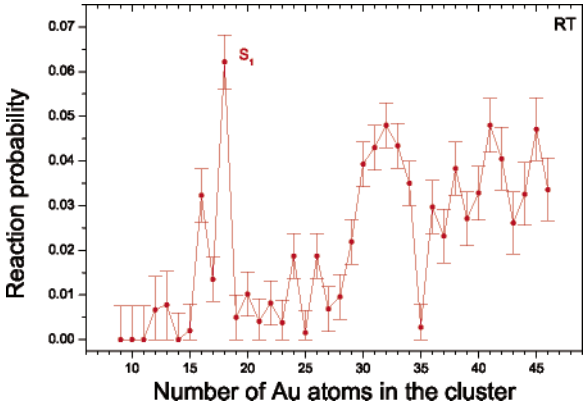

Figure 4. The reaction probability of Au_9-Au_{46} with the first CO molecule, S_1, for the source at RT.

Å. The radius of CO was taken to be 1.9 Å. The reaction probability is, thus, the reactive cross-section divided by this hard-sphere collision cross-section.

In collisions with CO molecules the clusters are scattered, which may cause deflection of clusters out of the beam and thus out of the detection region. To obtain accurate relative intensities of unreacted and reacted clusters of each cluster size, we must correct the intensities for the fraction deflected. The deflection probability per average collision, D, is determined by measuring the decrease in total amount of clusters, bare ones and reaction products, reaching the detection region as a function of the average number of collisions, i.e., reaction-cell pressure. The intensities of the $Au_n(CO)_m$ products are corrected for the fraction deflected in the reactive collision by dividing the intensity by $(1 - D)^m$. It is assumed that the ionization probability is equal for the bare and reacted clusters. If that was not the case, the result had been an apparently higher or lower deflection probability for the most reactive sizes, something that was not seen.

It should be noted that the sticking probability determined by comparing the relative abundance of pure and reacted clusters and fitting the first-order kinetic model depends on the formation of stable products and will thus be the combined probabilities of a cluster-molecule complex formation and this complex being sufficiently long-lived (10^{-4} s) to be detected.

Results

Figure 4 shows the reaction probabilities S_1 with the first CO molecule of Au_9-Au_{46} clusters, produced with the cluster source at RT. The error bars represent the uncertainties in fitting the kinetic model to the experimental data. They reflect the scattering of the results using different subsets of the data and are given as the upper limit in each size range. There is also an uncertainty in the absolute probability values of about 20% originating from the pressure measurement and deflection correction, which is size-independent or only weakly size-dependent and is not included in the error bars. The reaction probabilities S_i for $i > 1$ and the source at RT are all taken to be zero, as in the mass spectra of Au_n reacted with CO gas, no $Au_n(CO)_m$ complexes with $m > 1$ are observed. For the adsorption of the first CO molecule, a remarkable size dependence is measured, as can be seen in Figure 4. For clusters smaller than $n = 15$, no peaks that with certainty can be identified as reaction products are observed. Those clusters probably are unreactive or at least less reactive than can be observed due to the detection limit (~0.005) of the setup. It is improbable, but cannot be excluded, that the ionization potential

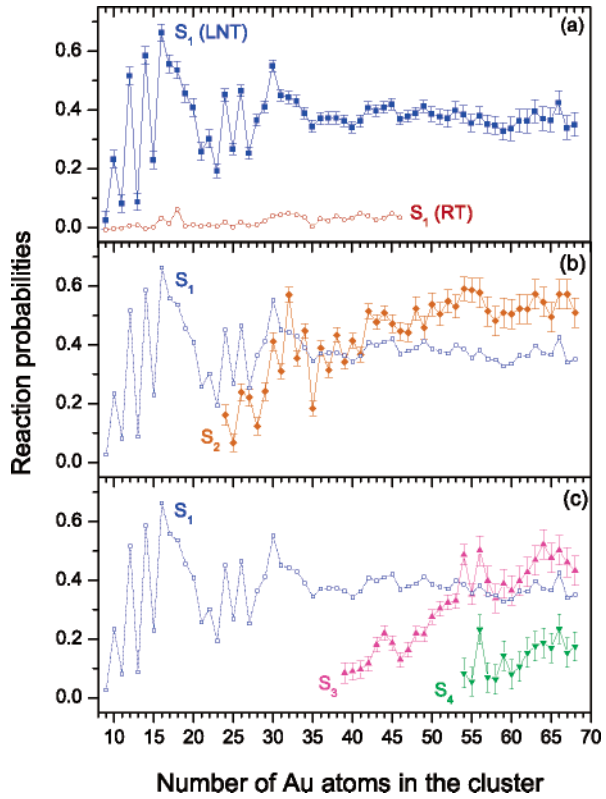

Figure 5. The reaction probability of Au_n ($n = 9-68$) clusters produced with the source at LNT for reactivity with CO molecules. (a) Reaction probability S_1 (■) with the first CO molecule at LNT. The corresponding S_1 values at RT (○), shown in Figure 3, are also added. (b) Reaction probabilities S_2 (◆) with the second CO molecule at LNT. The S_1 values at LNT (□) are added for comparison. (c) Reaction probabilities S_3 (▲) and S_4 (▼) with respectively the third and fourth CO molecule at LNT. The S_1 (□) values are also added.

of some reacted species, due to adsorption of a CO molecule, has increased and therefore has become higher than the employed photon energy of 7.89 eV, resulting in those species not being detected using the 157-nm ionization laser light. In the size range $n = 16-18$, the reactivity is much higher, and particularly high reactivity is observed for Au_{16} and Au_{18}. The reaction probability of the RT clusters in the size range $n = 19-28$ is overall very low, close to the detection limit, and possibly zero within the error estimates. The only exceptions to this are Au_{24} and Au_{26}, for which a low but measurable reactivity is observed. In the size range $n = 16-28$, also a pronounced odd−even staggering, even n clusters showing the highest reactivity, is found. For all Au_n clusters in the size range $n = 29-34$, there is a relatively high reaction probability with a local maximum for Au_{32}. A remarkably low reaction probability can be observed for Au_{35}. For larger cluster sizes, $n > 35$, again a relatively high reaction probability is found.

The reaction probabilities measured with the cluster source at LNT were found to be considerably higher, as indicated by Figure 5, showing the reaction probabilities of LNT gold clusters with CO molecules. First, comparing the reaction probabilities S_1 for the LNT clusters (Figure 5(a)) with the corresponding values for RT clusters (Figure 4, and also added to Figure 5(a)) reveals that clusters produced with the source at LNT are at least 10 times more reactive. Second, clusters of several sizes which appeared unreactive at RT form stable products on LNT clusters. Third, in contrast to RT clusters, adsorbing at most one CO molecule, LNT clusters can adsorb two, three, and even four CO molecules, as revealed by the reaction probabilities S_2, S_3, and S_4, shown in Figure 5(b) and (c).

Although the reactivity increases substantially upon cooling of the cluster source to LNT, the striking size selectivity for CO adsorption and the odd−even variations observed at RT are preserved at lower temperature. For the reaction probabilities S_1 (Figure 5(a)), we get the following size dependence. From $n = 10$ on, all clusters are reactive. Actually, a Au_8CO product could also be observed; however, the absence of the pure Au_8 peak, due to its too high ionization potential, did not allow reaction probability determination of the Au_8 cluster. Maxima in reaction probabilities S_1 are found in the size regions $n = 16-18$ and $n = 30-32$ and give rise to two humps located around the most reactive RT clusters Au_{16}, Au_{18}, and Au_{32}. Between those regions, odd−even staggering is found, as was also the case at RT.

Reaction probabilities S_2 are shown in Figure 5(b). We do not observe any $Au_n(CO)_2$ complexes for $n \leq 23$, but all clusters with more than 23 constituent atoms are clearly able to adsorb a second CO molecule. In the size range $n = 29-41$ striking odd−even variations can again be observed, showing a maximum for Au_{32}. An exceptionally low S_2 is measured for Au_{35}, the same size for which a low S_1 at RT was found. For larger clusters ($n > 41$) the size variation in S_2 is flattened, and for these cluster sizes, S_2 values higher than the corresponding S_1 values are observed.

The threshold sizes for adsorption of a third and a fourth CO molecule are around $n = 39$ and $n = 54$, respectively (Figure 5(c)). The main trend in the reaction probabilities S_3 and S_4 is the increase with increasing cluster size. In addition, some structure can be observed. The S_3 values show a hump around $n = 44$ and two enhanced values at 54 and 56, respectively. The reaction probability with the fourth CO molecule has a clear maximum for $n = 56$.

Discussion

A. Temperature Dependence of the CO Reactivity. A higher reactivity with lower temperatures is characteristic for a reaction where the reaction probability is limited by the stabilization of the reaction products. When the binding energy is low, a cluster-molecule complex can form, but it may decompose before detection if the thermal energy in the cluster is sufficiently high compared with the binding energy. This is particularly the case in our experiment where no stabilizing buffer gas is present and the chemisorption energy, the impact energy in the reactive collision, and any energy transferred in inelastic unreactive collisions need to be contained in the cluster.

The higher reactivity measured for clusters produced at LNT is consequently an effect of the lifetime of the cluster−molecule complexes being much longer than for the RT-produced clusters. Besides the fact that the initial internal energy is lower in the cluster, also the impact energy in the cluster−molecule collisions is lower. Other factors which also could contribute to the higher reaction probability of the cooler clusters are a higher initial trapping probability of the CO molecule and that a trapped molecule may have a longer residence time during which it can find an optimum binding site. Previous reports on CO adsorption on copper and gold clusters have led to the same conclusion that product stabilization can be a limiting factor.[46,66,69,80,81,84]

The observation of threshold sizes for stable binding of two, three, and four molecules, is typical for cases where the balance between the internal energy of the cluster and the adsorbate binding energy is critical. The adsorption of a molecule leads to an increase in the internal energy, which is reflected in a higher vibrational temperature. In a larger cluster with more vibrational degrees of freedom this temperature increase is

smaller, and thus more molecules can be adsorbed without reaching the temperature required for desorption of the CO molecule on the experimental time scale. In this context it is also understandable that there are more size-variations in a range close to the threshold size; for example, for clusters produced at LNT, S_1 has distinct variations for $n = 10-30$ and S_2 for $n = 24-40$, but less for larger sizes.

Since the adsorption of several molecules was not possible or less efficient on small clusters, it appears surprising that with increasing cluster size the reaction probability becomes higher for the second, and later also for the third molecule, than for the first one. This behavior can be seen in cases where isomers with high and low reactivity are present. In such a case S_1 would probe the average reactivity of the different isomers, whereas S_2 only probes the addition of a second molecule to the more reactive isomer. It is, however, not likely that for an extended size range there are more and less reactive isomers present in about the same fraction. One effect that we cannot exclude is the presence of a fraction of not well thermalized clusters. In the source, the clusters grow by picking up gold atoms or coalescence with other clusters. In this process the clusters are heated by the binding energy of the added gold atoms, but the collisions with the He atoms thermalize the clusters to the source temperature. There might however be a small fraction of clusters, which have picked up gold atoms just before exiting the source and did not have time to undergo the number of collisions with He atoms required to cool to the source temperature. The higher reaction probability with the second molecule could also be a real effect. After the adsorption of a molecule, the cluster is expected to have a dipole moment from the adsorbed CO molecule. In addition it could have a higher polarizability, as was predicted for copper clusters with CO adsorbed.[85] The increased polarizability and the dipole moment is expected to enhance the long-range interaction between the cluster and a CO molecule increasing the trapping probability. It was recently pointed out that the high oscillator strength of a CO molecule adsorbed onto a gold cluster was important for the efficiency of product stabilization by radiative cooling,[69] and with more molecules adsorbed the total emission efficiency should be higher. However, the time between reaction and detection is several orders of magnitude different between our experiment and that of Neumaier et al.[69] and radiative cooling is expected to play a smaller role in our case.

B. Size Dependence, Electronic Structure Effects, and Charge State Dependence. The size dependence of the reaction probabilities is, based on the conclusions from the temperature dependence, most likely reflecting a variation in product stability and, thus, CO adsorption energy of the different cluster sizes. The particularly high reaction probability of the RT-produced Au_{16}, Au_{18}, and Au_{32} presented in Figure 4 points at a correlation between reactivity and cluster electronic shell structure. When electron-counting rules are applied, it is assumed that CO molecules in a chemisorption process act as two-electron donors,[64,65,86] making the number of delocalized electrons in the reaction products $Au_{16}CO$, $Au_{18}CO$, and $Au_{32}CO$ equal to the magic numbers 18, 20, and 34, respectively, indicating that there is a tendency toward closed shell structures formation. Further analysis of the adsorption probability plots, especially Figure 4 and Figure 5(a), enabling direct comparison between RT and LNT conditions, reveals that the importance of electronic properties, found for the cluster source at RT, is preserved at lower temperatures. Evidence for this statement is the striking size dependence in the reaction probabilities at LNT (Figure 5(a)), showing high reactivity in the size regions $n = 16-18$ and $n = 30-32$, located around Au_{16}, Au_{18}, and Au_{32}, the most reactive RT clusters. Evidence for electronic properties governing size-dependent properties at both temperatures is also given by the occurrence of odd−even staggering as a function of the number of gold atoms, with even n species being more reactive. For these findings to be consistent with the expected enhanced stability of complexes with an even number of delocalized electrons, CO should indeed act as a two-electron donor.

In addition to the shell filling, also the symmetry of delocalized valence orbitals can enhance the adsorbate bond strength, an effect which was analyzed in an earlier study where the reactivity of neutral Cu_n clusters with CO was investigated.[81] A strong size selectivity, with Cu_{16} exhibiting the highest reactivity, was reported. Due to an efficient symmetry matching between the highest occupied molecular orbital (HOMO) of CO and the lowest unoccupied molecular orbital (LUMO) of a metal cluster two sizes below a shell closing, both having σ character, and between the HOMO of the cluster and the LUMO of CO having π character, efficient charge transfer (donation and back-donation, respectively) occurs, resulting in a high CO reaction probability.

The possibility that particular geometries or geometrical growth patterns are the reason for the size dependence of the CO reactivity should also be considered, even if it seems less likely. The binding energy of CO to different gold structures has been calculated,[87,88] and it was found that the binding energy was increasing when going from an extended low-index single-crystalline surface to a stepped surface or a small cluster. The higher binding energy at the low-dimensional structures was attributed to the presence of binding to low-coordinated gold atoms. An increasing CO binding energy with decreasing size down to 1.8 nm for gold clusters supported on TiO_2 has also been measured experimentally.[89] Using the argument that CO-bonding is stronger at low-coordinated sites, implies that planar structures would form more stable products than three-dimensional ones. However, the maximum in reactivity we observe for $Au_{16}-Au_{18}$ appears in a range where the transition from 2-D to 3-D structures is expected to have occurred.[10−13] There is also no obvious correlation between our measured reactivity and what could be expected for geometries proposed for Au_{20}[14] and Au_{32},[15] respectively. A tetragonal Au_{20} has four low-coordinated corner atoms, which could be expected to be good binding sites for CO, but Au_{20} does not show a particularly high reactivity in our experiment. The high reactivity measured for Au_{32} is difficult to explain by geometry arguments based on a cage-shaped cluster with only equivalent high-coordinated sites. In addition, with our present knowledge about gold clusters, it is much less likely that the odd−even staggering observed over extended size ranges could be attributed to geometry effects, than to the electronic structure. Still the individual geometry of each cluster will of course influence its ability to bind the CO molecule, but the main trends in the size-evolution of the CO reactivity have their origin in the electronic structure.

Since the interpretation that CO contributes two electrons to the shell filling is emanating from studies of gold cluster ions, it is interesting to compare our results with earlier studies of CO adsorption on gold clusters. There are several experimental investigations of CO reactivity with free gold clusters carried out by different groups. For neutral clusters, only CO adsorption onto the dimer was studied.[70] The CO adsorption on positive gold cluster ions has been investigated in ion trap experiments. There is one early study focusing on the characteristics around

the electronic shell closings of 8, 18, and 20, and it was found that Au_7^+ and Au_{19}^+ formed the most stable products.[64] In a more recent study Neumaier et al. have measured the CO adsorption on Au_n^+ up to $n = 65$.[69] For $n = 5-25$, all clusters react, with local maxima at $n = 7$, 15, 19, and 21. For larger clusters, only a few sizes, $n = 30$, 31, 32, 41, 48, and 49, are reactive. The reaction efficiency was interpreted in terms of a higher CO binding energy at the more reactive cluster sizes. The coinciding maxima at Au_7^+ and Au_{19}^+ are in agreement with the electron counting rules and the Au_{19}^+ cluster has the same number of valence electrons as the neutral Au_{18}, which we identify as the most reactive. However, in the study of Nygren et al. there is no indication of a high reactivity of Au_{17}^+, and Neumaier et al. find a local minimum at this size, being isoelectronic with neutral Au_{16}, for which we observe a high reactivity. Neither do the maxima at $n = 15$ and 21 coincide with maxima at the same sizes or their isoelectronic neutral counterparts of our study. The presence of reactive islands around Au_{31}^+, Au_{41}^+, and Au_{48}^+ is a very interesting observation, and we note that the first one of these overlaps with the $Au_{30}-Au_{34}$ range for which we measure a high reactivity.

There are several investigations of gold cluster anions reacting with CO. Two of them only include sizes smaller than were covered in our present study. Lee and Ervin measured the CO adsorption on Au_1^- to Au_7^- in a flow tube reactor in which He gas is present to stabilize the products.[46] They observe an increasing reactivity with increasing cluster size, and bimolecular rates show a reaction efficiency of up to a few percent, though the bimolecular rates were pressure-dependent, indicating that product stabilization through third-body collisions is critical. The study of Hagen et al.[66] only includes Au_1^- to Au_3^-, and thus direct comparisons with our results are difficult to make.

Wallace and Whetten measured the CO reactivity of Au_n^- up to $n = 19$ using a fast-flow reactor. They find almost all clusters reactive and measure a particularly high reactivity of Au_{11}^-, Au_{15}^-, and Au_{19}^-.[65] Balteanu et al. used an FT-ICR ion trap and covered the size range up to Au_{16}^- in their investigation of CO adsorption on gold cluster anions.[67] They find an enhanced reactivity of Au_7^- to Au_{11}^- with a distinct maximum at Au_{11}^-. The latter is in agreement with the finding of Wallace and Whetten, but no maximum at Au_{15}^- was observed by Balteanu et al. Our results do not indicate any particularly high reactivity neither for Au_{11} nor for Au_{12}. Au_{12} is at LNT more reactive than Au_{11} and Au_{13} but does not appear special compared with its even-numbered neighbors and does not have a measurable reactivity when produced at RT. One should however bear in mind that in this size range a transition from planar geometries to three-dimensional ones is expected.[10-13] This transition occurs at a larger size for the anions than for the cations, and although calculations predict the transition to occur at the same size for neutral and anionic clusters, this has not been verified experimentally. A reason for the lack of a corresponding maximum for the neutral $Au_{11/12}$ might thus be that the geometry and therefore also the electronic structure is fundamentally different. Au_{15}^- is isoelectronic with Au_{16}, so a high reactivity for these sizes is in agreement with models predicting stable products at clusters containing two electrons fewer than required for a shell closing. On the other hand, there is no indication of a high reactivity of Au_{17}^-, which would correspond to the maximum in reactivity/product stability of Au_{18} and Au_{19}^+. Instead, Wallace and Whetten measure a high reactivity of Au_{19}^-, which actually contains the same number of electrons as Au_{21}^+, displaying a high reactivity in the study of Neumaier et al. but also the same number of atoms as Au_{19}^+, exhibiting a high reactivity in both studies of cations.

Lee and Ervin,[46] Balteanu et al.,[67] and Neumaier et al.[69] report absolute values for the reaction probability or rate constants, but the comparison of our results with these numbers should be made with care since the conditions (temperature, collision energy, presence of buffer gas, and experimental time scale) are not the same in the different experiments. Lee and Ervin report rates corresponding to a reaction probability of single percent, which is similar to our values for RT-produced clusters. Somewhat higher values are reported for the most reactive cationic clusters in the study by Neumaier et al., who measure rate constants that are more than 10% of the Langevin rate constant. The reaction probabilities determined by Balteanu et al. are less than a tenth of a percent. This is a few orders of magnitude lower than we measure, although they inject clusters with an estimated temperature of about 40 K, which is even cooler than our LNT-produced clusters. However, they also report that they initially observe a higher reactivity, but it is reduced as the clusters are heated by multiple collisions in the trap. In an experiment where the binding energy controls the presence of stable products, the measured reactivity can be expected to be lower for the anions and higher for the cations due to polarization effects as predicted by Wu et al.[82]

The comparison between the CO adsorption onto different charge state gold clusters can be summarized as that there are several coinciding maxima at clusters with the same number of valence electrons, correlating to electron shell closures, but for the ionic clusters also additional local maxima are present. Although the maxima in almost all cases occur for even-electron clusters, it is only for the neutral clusters that we observe strong odd−even variations.

C. The Character of the Au−CO Bonding. The electronic shell model and electron counting rules are powerful in their simplicity, ability to provide a qualitative understanding, and applicability to extended size ranges, but for a deeper analysis and understanding of the cluster-molecule interaction more detailed models are required. Even though many properties exhibit a size dependence characteristic of an electronic shell structure, gold is not an ideal free-electron metal. An analysis of the electronic structure of gold clusters shows that there is a significant *s*−*d* hybridization also at levels close to the Fermi level.[11,17,90] It is expected that this presence of states with *d*-character close to the Fermi level enhances the bonding of CO.[87] For example, silver has compared to copper and gold lower lying *d*-states and less *s*−*d* hybridization, and in our experiment we do not observe any reaction (detection limit $S \approx 0.01$) between CO and Ag_n, neither did Lee and Ervin for Ag_n^-.[46] The *s*−*d* hybridization at the Fermi level has been calculated for individual cluster sizes,[11,90] but whether there is a systematic size dependence has to our knowledge not been investigated. However, in an analysis of photoelectron spectra of gold cluster cations it was concluded that for clusters with more than 20 atoms the location of the *d*-bands varied much less with cluster size than the location of the *s*-states and in particular of the HOMO level.[7] It is possible that a larger degree of *s*−*d* hybridization at the Fermi level of the even-electron clusters enhances the CO bonding of these species. Clusters with just-opened electronic shells, such as Au_9, Au_{21}, and Au_{35}, are expected to have a particularly high lying HOMO, and indeed these sizes are the least reactive or among the least reactive ones in their respective size range.

Detailed calculations of the size-dependent, as well as charge-state-dependent, CO adsorption have been made for Au_1-Au_6,[82]

clusters smaller than investigated in our experiment. The CO binding energy differs significantly for the different charge states, but no strong size-to-size fluctuations, similar to the odd−even staggering measured in our experiment, were found in the computational study. Highest binding energy was calculated for the cations, followed by the neutral clusters and the anions. However, the binding energy to the cationic clusters is decreasing with increasing size, while it is increasing for the anions, showing a converging trend with increasing size. From the ordering of the binding energy between the cation, neutral, and anion, the authors conclude that σ-bonding (forward donation) dominates over π-bonding (back-donation) as the main bonding mechanism. Even if there are no evident oscillations in the binding energy, an odd−even variation was calculated for the internal C−O vibrational frequency with a higher frequency calculated for CO bound to even-electron clusters compared to its odd-electron neighbors. A higher C−O vibrational frequency was also generally calculated for cationic Au_n, and a lower C−O vibrational frequency on anionic clusters, thus showing a correlation between high C−O vibrational frequency and a high CO adsorption energy. The higher frequency at the cationic complexes was attributed to a polarization effect.[91] This correlation between the vibrational frequency and the binding energy also points at the importance of the σ bonding in these small gold−CO complexes.

Besides measuring the reactivity of CO on gold cluster cations and experimentally determining the binding energy from an analysis of that data, Neumaier et al. also calculated binding energies for CO on Au_1^+−Au_8^+.[69] Superimposed on the trend with decreasing binding energy with increasing cluster size, they find a clear odd−even variation with a higher binding energy to the even-electron clusters. A detailed analysis of the origin of the odd−even variation was not provided, but the authors addressed the important issue of whether the clusters can be expected to adopt the lowest-energy isomer after reaction, and they concluded that the barriers involved were likely to be much smaller than the CO chemisorption energy. However, in a study of hydrogen addition to small gold clusters the formation route was thought to be of importance.[56] CO bonding to neutral Au_n up to size $n = 13$ has been calculated by Phala et al.[58] For the smaller clusters, the trends in binding energy with size are similar to the results of Wu et al.[82] For $n > 6$, the calculations were done for gold clusters with three-dimensional geometries. Neither in this size range the calculations predict any odd−even staggering for the binding energy, but there is a tendency that the odd−even variations in CO vibrational frequency continue. The authors suggest orbital overlap, rather than energetic matching between orbitals, being important for CO bonding to gold. This importance of the character of the frontier orbitals was also found in calculations for similar systems such as CO on Cu_n[85] and propene on Au_n,[59] where propene like CO acts as an electron donor. The molecule is found to bind most strongly to a site with matching orbital symmetries and/or where the orbitals protrude the most from the cluster. Thus, the local geometry of the electronic orbitals, rather than the atom locations, at the binding site is contributing to the potential of the cluster to bind a CO molecule. For the bonding of propene to the gold clusters it was found that the HOMO of propene interacted with the empty LUMO of the gold clusters, i.e., for odd-electron gold clusters there was no interaction with the singly occupied molecular orbital (SOMO). The physical reason for this was not clearified but a very good correlation between CO binding energy and LUMO orbital energy was found for cations, anions, and neutrals in the investigated size range up to $n = 5$. It would be interesting to analyze if the SOMO is similarly inactive in the CO bonding, since there are also differences between the CO and propene, the HOMO of the molecules have σ vs π character, and besides the forward donation from the HOMO of CO there is a significant back-donation of charge in the CO bonding. However, calculated binding energies of CO[82] and propene[59] on small gold clusters are very similar. Local geometry effects were also analyzed by Yuan and Zeng in a computational study of CO adsorption on Au_n^-, $n = 2-7$.[42] They found that the CO-bonding involved a net charge transfer to the molecule and low-coordinated Au atoms, initially having a large fraction of the excess negative charge, provided good binding sites for the CO molecules. However, the presence or absence of a particularly favorable binding site would not be enough to explain the size dependence we measure, since there is an overall good agreement between the size variations observed for the first and the second CO molecule.

As discussed there are several effects, such as orbital occupation number, $s-d$ hybridization and σ vs π bonding, which could give rise to an odd−even variation in CO binding energy, but the results presented here are not sufficient to determine their relative importance. In addition, it is not established that it actually is the optimum binding energy that controls the reactivity, particularly in view of most computational studies not finding an even−odd variation. It could for example be possible that a different degree of charge transfer or σ vs π interaction could affect the probability for the CO molecule to find its optimum binding site. Neither do we have the answer to why the odd−even variations are prominent for the neutral clusters but apparently absent for the ionic ones. A possibility could be that polarization and/or the direction of charge transfer is more similar from size to size for the ionic systems than for neutral clusters.

Conclusion

We have investigated the reactivity of neutral Au_n clusters with CO molecules with the cluster source kept at room or liquid nitrogen temperature. Although the observed reaction probabilities of cooled clusters are found to be much higher, attributed to a more efficient product stabilization at the lower temperature, a strong size selectivity is found for both temperatures of the cluster source. The size dependence is discussed qualitatively in terms of electronic shell structure. Apart from enhanced reactivities for Au_n clusters forming closed shell $Au_n(CO)_m$ structures, evidence for electronic properties of the produced species governing the size dependence of the reaction probabilities, is also given by odd−even staggering, observed as well at RT as at LNT. Detailed calculations of the electronic and geometric structures of the here studied $Au_n(CO)_m$ species would help to understand the reaction mechanisms and hopefully clarify issues such as the contribution of the carbon lone pair electrons to the electronic shells, the relative importance of σ and π bonding, the role of the SOMO in the odd-electron clusters, the influence of $s-d$ hybridization, and the character of the local adsorption sites.

Our results show both similarities and differences with CO adsorption measured on gold cluster anions and cations. There is generally a better agreement if one compares the number of valence electrons rather than the number of atoms, and electronic shell effects show up for all charge states. However, all maxima are not reproduced for both neutral, anionic, and cationic clusters, and the strong odd−even variations we observe for neutral Au_n were not present in the measurements on ionic

clusters. This comparison demonstrates the importance of the availability of data for clusters in different charge states, as well as of experimental configurations with different reaction conditions, to obtain a more complete description of the reaction.

Acknowledgment. This work is supported by the Fund for Scientific Research−Flanders (FWO), the Flemish Concerted Action (GOA/2004/02), and the Belgian Interuniversity Poles of Attraction (IAP) program. N.V. was Belgian Erasmus exchange student in Göteborg, Sweden. Encouraging discussions with Prof. Arne Rosén have been greatly appreciated.

References and Notes

(1) Ekardt, W. *Phys. Rev. B* **1984**, *29*, 1558.
(2) Knight, W. D.; Clemenger, K.; de Heer, W. A.; Saunders: W. A.; Chou, M. Y.; Cohen, M. L. *Phys. Rev. Lett.* **1984**, *52*, 2141.
(3) de Heer, W. A. *Rev. Mod. Phys.* **1993**, *65*, 611.
(4) Katakuse, I.; Ichihara, T.; Fujita, Y.; Matsuo, T.; Sakurai, T.; Matsuda, H. *Int. J. Mass Spectrom. Ion Proc.* **1985**, *67*, 229.
(5) Katakuse, I.; Ichihara, T.; Fujita, Y.; Matsuo, T.; Sakurai, T.; Matsuda, H. *Int. J. Mass Spectrom. Ion Proc.* **1986**, *74*, 33.
(6) Neukermans, S.; Janssens, E.; Tanaka, H.; Silverans, R. E.; Lievens, P. *Phys. Rev. Lett.* **2003**, *90*, 033401.
(7) Taylor, K. L.; Pettiette-Hall, C. L.; Cheshnovsky, O.; Smalley, R. E. *J. Chem. Phys.* **1992**, *96*, 3319.
(8) Jackschath, C.; Rabin, I.; Schulze, W. *Ber. Bunsen-Ges. Phys. Chem.* **1992**, *96*, 1200.
(9) Collings, B. A.; Athanassenas, K.; Lacombe, D.; Rayner, D. M.; Hackett, P. A. *J. Chem. Phys.* **1994**, *101*, 3506.
(10) Furche, F.; Ahlrichs, R.; Weis, P.; Jacob, C.; Gilb, S.; Bierweiler, T.; Kappes, M. M. *J. Chem. Phys.* **2002**, *117*, 6982.
(11) Häkkinen, H.; Moseler, M.; Landman, U. *Phys. Rev. Lett.* **2002**, *89*, 033401.
(12) Häkkinen, H.; Yoon, B.; Landman, U.; Li, X.; Zhai, H.-J.; Wang, L.-S. *J. Phys. Chem. A* **2003**, *107*, 6168.
(13) Xiao, L.; Wang, L. *Chem. Phys. Lett.* **2004**, *392*, 452.
(14) Li, J.; Li, X.; Zhai, H.-J.; Wang, L.-S. *Science* **2003**, *299*, 864.
(15) Johansson, M. P.; Sundholm, D.; Vaara, J. *Angew. Chem., Int. Ed.* **2004**, *43*, 2678.
(16) Garzón, I. L.; Beltrán, M. R.; González, G.; Gutíerrez-González, I.; Michaelian, K.; Reyes-Nava, J. A.; Rodríguez-Hernández, J. I. *Eur. Phys. J. D* **2003**, *24*, 105.
(17) Häkkinen, H.; Moseler, M.; Kostko, O.; Morgner, N.; Austruc Hoffman, M.; v. Issendorf, B. *Phys. Rev. Lett.* **2004**, *93*, 093401.
(18) Haruta, M. *Catal. Today* **1997**, *36*, 153.
(19) Bond, G. C.; Thompson, D. T. *Catal. Rev. Sci. Eng.* **1999**, *41*, 319.
(20) Choudhary, T. V.; Goodman, D. W. *Top. Catal.* **2002**, *21*, 25.
(21) Haruta, M. *Chem. Record* **2003**, *3*, 75.
(22) Hutchings, G. J. *Gold Bull.* **2004**, *37*, 3.
(23) Valden, M.; Lai, X.; Goodman, D. W. *Science* **1998**, *281*, 1647.
(24) Sanchez, A.; Abbet, S.; Heiz, U.; Schneider, W. D.; Häkkinen, H.; Barnett, R. N.; Landman, U. *J. Phys. Chem. A* **1999**, *103*, 9573.
(25) Kozlov, A. I.; Kozlova, A. P.; Liu, H.; Iwasawa, Y. *Appl. Catal. A* **1999**, *182*, 9.
(26) Schubert, M. M.; Hackenberg. S.; van Veen, A. C.; Muhler, M.; Plzak, V.; Behm, R. J. *J. Catal.* **2001**, *197*, 113.
(27) Wolf, A.; F. Schüth, F. *Appl. Catal. A* **2002**, *226*, 1.
(28) Gluhoi, A. C.; Dekkers, M. A. P.; Nieuwenhuys, B. E. *J. Catal.* **2003**, *219*, 197.
(29) Costello, C. K.; Yang, J. H.; Law, H. Y.; Wang, Y.; Lin, J.-N.; Marks, L. D.; Kung, M. C.; Kung, H. H. *Appl. Catal. A* **2003**, *243*, 15.
(30) Fu, Q.; Saltsburg, H.; Flytzani-Stephanopoulos, M. *Science* **2003**, *301*, 935.
(31) Sinha, A. K.; Seelan, S.; Tsubota, S.; Haruta, M. *Top. Catal.* **2004**, *29*, 95.
(32) Lee, S.; Fan, C.; Wu, T.; Anderson, S. L. *J. Am. Chem. Soc.* **2004**, *126*, 5682.
(33) Häkkinen, H.; Abbet, S.; Sanchez, A.; Heiz, U.; Landman, U. *Angew. Chem., Int. Ed.* **2003**, *42*, 1297.
(34) Liu, Z.-P.; Gong, X.-Q.; Kohanoff, J.; Sanchez, C.; Hu, P. *Phys. Rev. Lett.* **2003**, *91*, 266102.
(35) Molina, L. M.; Hammer, B. *Phys. Rev. B* **2004**, *69*, 155424.
(36) Molina, L. M.; Rasmussen, M. D.; Hammer, B. *J. Chem. Phys.* **2004**, *120*, 7673.
(37) Broqvist. P.; Molina, L. M.; Grönbeck, H.; Hammer, B. *J. Catal.* **2004**, *227*, 217.
(38) Häkkinen, H.; Landman, U. *J. Am. Chem. Soc.* **2001**, *123*, 9704.
(39) Wallace, W. T.; Whetten, R. L. *J. Am. Chem. Soc.* **2002**, *124*, 7499.
(40) Hagen, J.; Socaciu, L. D.; Elijazyfer, M.; Heiz, U.; Bernhardt, T. M.; Wöste, L. *Phys. Chem. Chem. Phys.* **2002**, *4*, 1707.
(41) Wells, D. H., Jr.; Delgass, W. N.; Thomson, K. T. *J. Catal.* **2004**, *225*, 69.
(42) Yuan, D. W.; Zeng, Z. *J. Chem. Phys.* **2004**, *120*, 6574.
(43) Socaciu, L. D.; Hagen, J.; Bernhardt, T. M.; Wöste, L.; Heiz, U.; Häkkinen, H.; Landman, U. *J. Am. Chem. Soc.* **2003**, *125*, 10437.
(44) Kimble, M. L.; Castleman, A. W., Jr.; Mitrić, R.; Bürgel, C.; Bonačić-Koutecký, V. *J. Am. Chem. Soc.* **2004**, *126*, 2526.
(45) Cox, D. M.; Brickman, R.; Creegan, K.; Kaldor, A. *Z. Phys. D* **1991**, *19*, 353.
(46) Lee, T. H.; Ervin, K. M. *J. Phys. Chem.* **1994**, *98*, 10023.
(47) Salisbury, B. E.; Wallace, W. T,; Whetten, R. L. *Chem. Phys.* **2000**, *262*, 131.
(48) Kim, Y. D.; Fischer, M.; Ganteför, G. *Chem. Phys. Lett.* **2003**, *377*, 170.
(49) Mills, G.; Gordon, M. S.; Metiu, H. *Chem. Phys. Lett.* **2002**, *359*, 493.
(50) Wells, D. H., Jr.; Delgass, W. N.; Thomson, K. T. *J. Chem. Phys.* **2002**, *117*, 10597.
(51) Yoon, B.; Häkkinen, H.; U. Landman, U. *J. Phys. Chem. A* **2003**, *107*, 4066.
(52) Wallace, W. T.; Wyrwas, R. B.; Whetten, R. L.; Mitrić, R.; Bonačić-Koutecký, V. *J. Am. Chem. Soc.* **2003**, *125*, 8408.
(53) Sun, Q.; Jena, P.; Kim, Y. D.; Fischer, M.; Ganteför, G. *J. Chem. Phys.* **2004**, *120*, 6510.
(54) Sugawara, K.; Sobott, F.; Vakhtin, A. B. *J. Chem. Phys.* **2003**, *118*, 7808.
(55) Varganov, S. A.; Olson, R. M.; Gordon, M. S.; Mills, G.; Metiu, H. *J. Chem. Phys.* **2004**, *120*, 5169.
(56) Fisher, D.; Andreoni, W.; Curioni, A.; Grönbeck, H.; Burkart, S.; Ganteför, G. *Chem. Phys. Lett.* **2002**, *361*, 389.
(57) Buckart, S.; Ganteför, G.; Kim, Y. D.; Jena, P. *J. Am. Chem. Soc.* **2003**, *125*, 14205.
(58) Phala, N. S.; Klatt, G.; van Steen, E. *Chem. Phys. Lett.* **2004**, *395*, 33.
(59) Chrétien, S.; Gordon, M. S.; Metiu, H. *J. Chem. Phys.* **2004**, *121*, 3756.
(60) Knickelbein, M. B.; Koretsky, G. M. *J. Phys. Chem. A* **1998**, *102*, 580.
(61) Dietrich, G.; Krückeberg, S.; Lützenkirchen, K.; Schweikhard, L.; Walther, C. *J. Chem. Phys.* **2000**, *112*, 752.
(62) Rousseau, R.; Marx, D. *J. Chem. Phys.* **2000**, *112*, 761.
(63) Koretsky, G. M.; Knickelbein, M. B.; Rousseau, R.; Marx, D. *J. Phys. Chem. A* **2001**, *105*, 11197.
(64) Nygren, M. A.; Siegbahn, P. E. M.; C. Jin, C.; Guo, T.; Smalley, R. E. *J. Chem. Phys.* **1991**, *95*, 6181.
(65) Wallace, W. T.; Whetten, R. L. *J. Phys. Chem. B* **2000**, *104*, 10964.
(66) Hagen. J.; Socaciu, L. D.; Heiz, U.; Bernhardt, T. M.; Wöste, L. *Eur. Phys. J. D* **2003**, *24*, 327.
(67) Balteanu, I.; Balaj, O. P.; Fox, B. S.; Beyer, M. K.; Bastl, Z.; Bondybey, V. E. *Phys. Chem. Chem. Phys.* **2003**, *5*, 1213.
(68) Kimble, M. L.; Castleman, A. W., Jr. *Int. J. Mass Spectrom.* **2004**, *233*, 99.
(69) Neumaier, M.; Weigend, F.; Hampe, O.; Kappes, M. M. *J. Chem. Phys.* **2005**, *122*, 104702.
(70) Lian, L.; Hackett, P. A.; Rayner, D. M. *J. Chem. Phys.* **1993**, *99*, 2583.
(71) Morse, M. D.; Geusic, M. E.; Heath, J. R.; Smalley, R. E. *J. Chem. Phys.* **1985**, *83*, 2293.
(72) Cox, D. M.; Reichman, K. C.; Trevor, D. J.; Kaldor, A. *J. Chem. Phys.* **1988**, *88*, 111.
(73) Guo, B. C.; Kerns, K. P.; Castleman, A. W., Jr. *J. Chem. Phys.* **1992**, *96*, 8177.
(74) Ren, X.; Hintz, P. A.; Ervin, K. M. *J. Chem. Phys.* **1993**, *99*, 3575.
(75) Holmgren, L.; Andersson, M.; Rosén, A. *Surf. Sci.* **1995**, *331*−*333*, 231.
(76) Andersson. M.; Holmgren, L.; Rosén, A. *Surf. Rev. Lett.* **1996**, *3*, 683.
(77) Holmgren, L.; Rosén, A. *J. Chem. Phys.* **1999**, *110*, 2629.
(78) Balteanu, I.; Achatz, U.; Balaj, P.; Fox, B. S.; Beyer, M. K.; Bondybey, V. E. *Int. J. Mass Spectrom.* **2003**, *229*, 61.
(79) Cox, D. M.; Trevor, D. J.; Whetten. R. L.; Kaldor, A. *J. Phys. Chem.* **1988**, *92*, 421.
(80) Leuchtner, R. E.; Harms, A. C.; Castleman, A. W., Jr. *J. Chem. Phys.* **1990**, *92*, 6527.
(81) Holmgren, L.; Grönbeck, H.; Andersson, M.; Rosén, A. *Phys. Rev. B.* **1996**, *53*, 16644.
(82) Wu, X.; Senapati, L.; Nayak, S. K.; Selloni, A.; Hajaligol, M. *J. Chem. Phys.* **2002**, *117*, 4010.
(83) Andersson, M.; Persson, J. L.; Rosén, A. *J. Phys. Chem.* **1996**, *100*, 12222.

(84) Wallace, W. T.; Whetten, R. L. *Eur. Phys. J. D* **2001**, *16*, 123.
(85) Cao, Z.; Wang, Y.; Zhu, J.; Wu, W.; Zhang, Q. *J. Phys. Chem. B* **2002**, *106*, 9649.
(86) Nygren, M. A.; Siegbahn, P. E. M. *J. Phys. Chem.* **1992**, *96*, 7579.
(87) Lopez, N.; Janssens, T. V. W.; Clausen, B. S.; Xu, Y.; Mavrikakis, M.; Bligraard, T.; Nørskov, J. K. *J. Catal.* **2004**, *223*, 232.
(88) Piccolo, L.; Loffreda, D.; Cadete Santos Aires, F. J.; Deranlot, C.; Jugnet, Y.; Sautet, P.; Bertolini, J. C. *Surf. Sci.* **2004**, *556*−*558*, 995.
(89) Meier, D. C.; Goodman, D. W. *J. Am. Chem. Soc.* **2004**, *126*, 1892.
(90) Grönbeck, H.; Broqvist, P. *Phys. Rev. B*, **2005**, *71*, 073408.
(91) Lupinetti, A. J.; Fau, S.; Frenking, G.; Strauss, S. H. *J. Phys. Chem. A* **1997**, *101*, 9551.